Field-cycling NMR relaxometry of a liquid crystal above T_{NI} in mesoscopic confinement

P. J. Sebastião,[1,2,*] D. Sousa,[3] A. C. Ribeiro,[1,2] M. Vilfan,[4,†] G. Lahajnar,[4] J. Seliger,[4,5] and S. Žumer[4,5]
[1]*Centro de Física da Matéria Condensada, Av. Prof. Gama Pinto 2, 1649-003 Lisbon, Portugal*
[2]*Department of Physics, Technical University of Lisbon, Av. Rovisco Pais, 1049-001 Lisbon, Portugal*
[3]*Technical University of Lisbon, IST/SMEEP, Av. Rovisco Pais, 1049-001 Lisbon, Portugal*
[4]*Jozef Stefan Institute, Jamova 39, SI-1000 Ljubljana, Slovenia*
[5]*Department of Physics, University of Ljubljana, Jadranska 19, SI-1000 Ljubljana, Slovenia*
(Received 17 May 2005; published 14 December 2005)

We measured the proton spin-lattice relaxation times in the isotropic phase of liquid crystal 4′-*n*-pentyl-4-cyanobiphenyl (5CB) confined into porous glass (CPG) with the average pore diameter ~72 nm. The analysis of T_1^{-1} frequency dispersions, spanning over four decades, shows that the main relaxation mechanism induced by the ordered surface layer are molecular reorientations mediated by translational displacements (RMTD). The RMTD contribution to T_1^{-1} is proportional to the inverse square root of Larmor frequency, a consequence of the equipartition of diffusion modes along the surface. Low and high frequency cutoffs of the RMTD mechanism clearly reveal that the surface alignment of liquid crystal is random planar with the size of uniformly oriented patches ~5 nm, depending on the treatment of the CPG matrix. According to the size of the uniformly oriented patches varies also the thickness of the ordered surface layer and its temperature behavior. The surface-induced order parameter is found to be temperature independent and determined by the local short range surface interactions.

DOI: 10.1103/PhysRevE.72.061702 PACS number(s): 61.30.Hn, 61.30.Pq, 33.25.+k, 76.60.−k

I. INTRODUCTION

Field-cycling relaxometry is a powerful nuclear magnetic resonance (NMR) technique for the identification and characterization of molecular dynamics in complex fluids, porous media, and liquid-solid interfaces [1]. It allows, by measuring the frequency dependence of relaxation times, an insight into a broad dynamic range spanning over the kilohertz and the low megahertz regime. When applied to liquid crystals, the field-cycling NMR relaxometry clearly shows specific features of different mesophases. For example, in the nematic phase the proton spin-lattice relaxation rate in the kHz range is proportional to the inverse square root of the Larmor frequency, $T_1^{-1} \sim \omega^{-1/2}$ [2]. The underlying dynamic processes are collective orientational fluctuations, known as order director fluctuations (ODFs). Their spectrum covers a broad frequency range, but their relative contribution to the overall relaxation dominates at kHz frequencies, where the effects of fast individual molecular motions are negligible. The characteristic exponent $-1/2$ is related to the three-dimensional nature of fluctuations in the nematic phase. The dispersion behavior is different in smectic phases, where the layered structure supports mainly two-dimensional layer undulations. They lead—as long as the interaction between layers is negligible—to a linear dependence of the relaxation time on the Larmor frequency, $T_1^{-1} \sim \omega^{-1}$. The linear behavior has been definitely observed in the multilamellar dispersions and vesicles formed by lyotropic liquid crystals [3–7], but there are some doubts about the capability of NMR to detect layer undulations in the thermotropic analogs [8]. In the tilted smectic *C* phase, the contributions of both mechanisms, layer undulations and three-dimensional azimuthal fluctuations, were reported [9]. Yet, irrespective of the underlying liquid crystalline state, the onset of the isotropic phase above T_{NI} is always accompanied by the disappearance of T_1^{-1} frequency dependence below 10 MHz. This indicates that the proton relaxation mechanisms in the isotropic phase are fast motions with correlation times shorter than $\sim 10^{-8}$ s. Only in the immediate vicinity of the phase transition, a weak effect of order fluctuations appears in the kHz range [2].

In this paper we apply the proton field-cycling NMR relaxometry to the isotropic phase of a nematic liquid crystal confined into cavities of mesoscopic size. It is well known that the confinement has a strong impact on the spin relaxation in the nematic phase. This is merely due to the complex director field imposed by the surface-liquid-crystal interactions, elastic forces, and morphology of the cavity [10]. The intrinsic effects of confinement are properly observed in cavities with inorganic walls, i.e., in the absence of cross relaxation between the protons of the liquid crystal and those of the solid matrix [11,12]. Terekhov *et al.* studied a nematic confined into porous glasses and pointed out that an increase in the spin-lattice relaxation rate, larger in smaller pores, is due to molecular reorientations induced by translational diffusion [13]. At variance, Leon *et al.* argue that the relaxation of the nematic phase in aerogel nanocavities reveals the fractal nature of the inner surfaces as shown by the characteristic dispersion exponent, −0.67 instead of −0.5, as in the bulk nematic phase [14].

The impact of spatial confinement is clearly visible also in the isotropic phase where the spin-lattice relaxation shows strong frequency dispersion in the kHz range, quite opposite to the flat dispersion curve of the bulk [15–17]. In fact, the isotropic phase of a liquid crystal in cavities of mesoscopic

*Electronic address: pedros@lince.cii.fc.ul.pt
†Electronic address: mika.vilfan@ijs.si

size is not truly isotropic throughout the cavity. Most of the solid surfaces induce a certain degree of orientational order in a thin layer of liquid crystal next to the surface at temperatures far above T_{NI}, where the bulk turns into the isotropic phase. The orientation of molecular director in the surface layer is either planar, tilted, or homeotropic. The planar alignment can be further characterized as uniform, with long molecular axes oriented in one direction in the plane, or random. According to the Landau–de Gennes theory, the order parameter is the largest next to the surface (S_0) and decays then exponentially with increasing distance from the wall in the case of surfaces that induce homeotropic or uniform planar alignment [18]. The characteristic decay constant is the nematic correlation length ξ which exhibits a strong pretransitional increase on approaching T_{NI} from above. Taking into account the finite length of molecules, Crawford *et al.* found a more realistic order parameter profile which is constant over a molecular distance l_0 from the wall and only then starts to decrease exponentially with the decay constant ξ [19]. Later, some homeotropic cases were reported where the thin layer with constant order parameter has not only orientational but also positional, i.e., presmectic order. The coupling between the orientational and positional order results in an enhanced degree of orientational order in the layer with constant order parameter and leads to an abrupt decrease in the orientational order at the border between this layer and the "attached" exponentially decaying part [20–22]. In the case of random planar anchoring, the thickness of the ordered layer is expected to be smaller than the nematic correlation length and dependent on the size of uniformly oriented patches.

Despite the ordered layer at the surface, the nematic-isotropic transition is discontinuous in cavities which are considerably larger than the thickness of the ordered layer (it is understood that the term "isotropic" in this context is used to describe the high-temperature phase with a weakly ordered surface layer and isotropic interior volume of the cavity). The situation is different in cases where the nematic correlation length is of the order of the cavity size. Here the discontinuous transition is suppressed and replaced by a continuous evolution of order with decreasing temperature. The critical cavity size, separating both regimes, depends on the type and strength of the surface anchoring and on the size and topology of the cavity [23,24].

In view of the strong effect of the confinement on the proton relaxation in the isotropic phase, it is expected that NMR relaxometry can provide an insight into the onset and nature of the surface-induced order. Such information is relevant particularly in view of the recent experimental findings, which indicate that the onset of orientational order with decreasing temperature might take place in a rather complex manner [25,26]. In the present study we measured and analyzed the proton spin-lattice relaxation of the liquid crystal 4′-*n*-pentyl-4-cyanobiphenyl (5CB) confined in the controlled porous glass (CPG) with the average pore diameter ~72 nm. Liquid crystal 5CB—the most extensively studied nematic liquid crystal up to now—has been chosen as a representative of the alkyl-cyanobiphenyl family whose members are frequently applied in LCD optical devices. We expect that the results obtained for 5CB will be relevant also for other nematogenic compounds [27,28]. The CPG glass with randomly oriented and interconnected pores of mesoscopic size is a convenient host matrix. The cavities are, on the one hand, small enough to show significant effects of the confinement, and on the other hand, sufficiently large to retain the bulklike isotropic phase some distance away from the walls. Consequently, they show the effects of the liquid-crystal-surface interactions, unbiased by the finite-size effects.

The purpose of the present work is to investigate the proton spin-lattice relaxation mechanisms in the isotropic phase of confined 5CB and to assess information on the surface-induced order and its impact on molecular dynamics upon confinement. In contrast to previous relaxometry studies [15,16], where the effect of confinement was only qualitatively indicated, we present a quantitative analysis of T_1^{-1} dispersions at different temperatures. Our primary issue is to investigate the effect of molecular translational diffusion on the spin relaxation, which depends on the spatial profile of the surface-induced order, orientation of the surface director, and on the topological structure of the cavity. In this way, proton NMR relaxometry can be considered as a complementary method to dielectric spectroscopy, which has been applied to 5CB and its higher homologue 8CB in cavities of similar size [28–31]. The advantage of dielectric spectroscopy in the MHz frequency range is to detect precisely 180° molecular reorientations, which do not affect NMR parameters. On the other hand, restricted tumbling of molecules around the short axis is observable by both methods, whereas the translational diffusion affects primarily NMR spin relaxation times.

The disposition of the paper is as follows. In Sec. II we describe the experiment and present the measurements of the proton spin-lattice relaxation rates T_1^{-1} in the frequency range from 10 kHz to 100 MHz. In the next section, the effect of confining surfaces on the relaxation rate is formulated and the corresponding frequency and temperature dependences of T_1^{-1} are predicted. In Sec. IV, experimental data are quantitatively analyzed in terms of the bulk and surface-induced relaxation mechanisms. The origin and characteristics of the additional relaxation mechanisms that appear upon confinement are discussed. The fitted parameters throw some light on the structure and nature of the ordered layer and lead to the conclusion that the order of 5CB at the surface of porous glass is random planar with the size of uniformly oriented patches depending on the treatment of the CPG matrix. A summary is given in Sec. V.

II. EXPERIMENT

Liquid crystal under study is the common 5CB, purchased from Frinton Laboratories, New Jersey, and used without further purification. Its nematic phase extends from 24 to 35 °C in the bulk. Controlled-pore glass (CPG Inc., New Jersey), used as the confining solid matrix, consists of porous grains with randomly oriented and strongly interconnected voids of roughly cylindrical shape (Fig. 1). The average diameter of voids is ~72 nm and the corresponding pores' volume 0.75 cm^3/g; the size of the grains ranges from 200 to

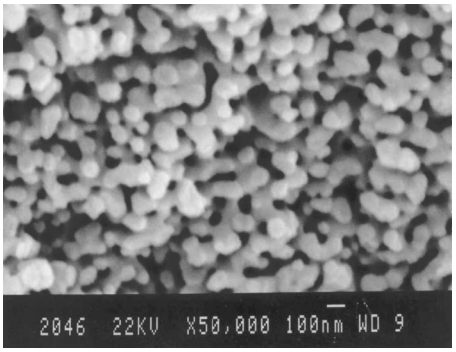

FIG. 1. Scanning electron micrograph (SEM) of the controlled-pore-glass (CPG) with average pore diameter ~72 nm. Micrograph provided by the Ceramics Department, J. Stefan Institute.

800 μm. As proved by the atomic force microscopy, the surface of the voids is smooth down to the nanometer scale [32]. From the chemical point of view, the CPG surface contains OH^- groups and is hydrophilic. In preparing the sample for the NMR measurements, the CPG was cleaned by soaking the grains into a mixture of concentrated sulphuric and nitric acids, followed by the extensive washing with distilled, de-ionized water until a neutral *p*H was obtained. The CPG grains were then set under modest vacuum and dried for 24 h at 200 °C. During the filling procedure an amount of isotropic 5CB, matching the volume of the pores, was soaked into CPG grains. The material was then immediately transferred into a NMR tube, set under vacuum at a temperature where 5CB is isotropic, and sealed. For comparison, using a somewhat different treatment of the CPG matrix another sample was prepared, i.e., CPG was dried at 300 °C before the filling with the liquid crystal. Hereafter the sample with CPG dried at 200 °C will be denoted as sample 1 and the other one as sample 2.

We found that the nematic-isotropic transition in the confined 5CB takes place within ~1 K below the bulk T_{NI} in agreement with earlier reports [33]. Up to now there has been no conclusive evidence whether the preferred orientation of liquid crystal molecules at the nontreated CPG walls is uniformly planar, randomly planar, or oblique to the surface. On the other hand, the potential effects of the magnetic field can be safely ruled out as the magnetic coherence length is about one order of magnitude larger than the size of the voids.

The proton spin-lattice relaxation times of 5CB in the confined and in the bulk state have been measured as a function of Larmor frequency and temperature above T_{NI}. In order to cover the frequency range from a few kilohertz to 100 MHz, two different NMR spectrometers were used: a Bruker SXP-4/100 for frequencies between 5 and 100 MHz, and a home-built fast field-cycling spectrometer in the low frequency regime [34]. In the MHz regime, the usual inversion-recovery pulse sequence was used to obtain the T_1 data. On the field-cycling spectrometer, the sequence $B_{\mathrm{H}\to\mathrm{L}}-\tau_i-B_{L\to H}-\pi/2-\mathrm{FID}$ was applied, where τ_i is the evolution time, $\pi/2$ is the radio-frequency pulse, and $B_{H\to L}$ and $B_{L\to H}$ are transitions between the high and low magnetic fields, respectively. At 5 MHz, i.e., at the "meeting point" of the two techniques, a good agreement between the T_1 values of bulk 5CB measured by the conventional and by the field-cycling spectrometer was established. The time dependence of the magnetization curves was a monoexponential function in all experiments indicating a uniform spin-lattice relaxation time throughout the sample. All measurements were performed upon heating the sample first well into the isotropic phase and then cooling it to the desired temperature for the measurement. The experimental error of spin-lattice relaxation measurements is estimated to be less than ±10%.

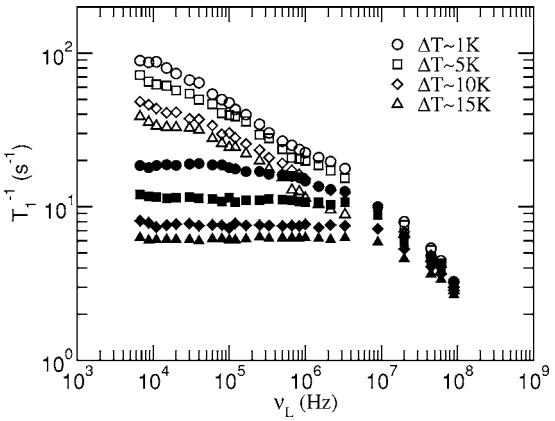

FIG. 2. Frequency dispersion of proton spin-lattice relaxation rate T_1^{-1} of 5CB in the porous glass (sample 1, open symbols) and in the bulk (solid symbols) at four temperatures above the nematic-isotropic transition temperature T_{NI} ($\Delta T=T-T_{NI}$).

The frequency dependences of the proton spin-lattice relaxation rates T_1^{-1} of confined 5CB, recorded at four different temperatures in the isotropic phase, are shown in Fig. 2. For comparison, the T_1^{-1} values of the bulk 5CB are also plotted in the figure. It is clearly seen that the difference between the values of the confined and bulk relaxation rates increases with decreasing frequency. Whereas the bulk relaxation rates, apart from the measurements at ~1 K above the transition, show a pronounced dispersion only in the MHz frequency range, the T_1^{-1} data of the confined 5CB significantly increase with decreasing frequency in the kHz range. Eventually, a levelling-off occurs below 10^4 Hz. This fact suggests that the confinement induces at least one additional relaxation mechanism with characteristic frequency in the kHz range. The temperature dependences of T_1^{-1}, measured at 11 kHz, are presented for the two confined samples and bulk 5CB in Fig. 3. The enhancement of the relaxation rate upon confinement is observed in the whole frequency interval of ~25 K above T_{NI}. In sample 2, containing the CPG matrix dried at a higher temperature, the relaxation is faster and shows a stronger pretransitional effect.

III. RELAXATION MECHANISMS IN THE CONFINED ISOTROPIC PHASE

Proton spin-lattice relaxation is induced by the time-varying magnetic dipole-dipole interaction between two neighboring proton spins. In the bulk isotropic phase, the time variation of spin interactions occurs due to fast molecular motions which include conformational changes, local ro-

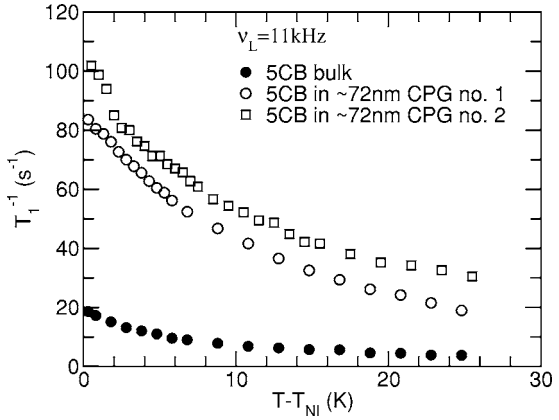

FIG. 3. Temperature dependence of proton spin-lattice relaxation rate T_1^{-1} at Larmor frequency ν=11 kHz for 5CB in porous glass (sample 1 and sample 2) and in the bulk.

tations, and short translational displacements of spin-bearing molecules [35,36]. Close to the transition into the nematic phase, order fluctuations (OFs), reflected in the onset and decay of weakly ordered clusters, take a pronounced part in the relaxation process as well. The measurements of the bulk spin-lattice relaxation rate in the frequency range below 100 MHz—which are relevant for a comparison with the confined 5CB data in the present study—are not able to discern unambiguously among different relaxation mechanisms. Yet the relaxation rate can be well fitted by a superposition of two contributions of the BPP (Bloembergen, Purcell, Pound) type,

$$\left(\frac{1}{T_1}\right)_{BPP} = A\left[\frac{\tau_c}{1+\omega^2\tau_c^2} + \frac{4\tau_c}{1+4\omega^2\tau_c^2}\right]. \tag{1}$$

One of them is characterized by the correlation time τ_c of the order of 10^{-10} s and the other by $\tau_c \sim 10^{-9}$ s. The contribution with the shorter correlation time may be reasonably ascribed to the joined effect of conformational changes and rotations around the long molecular axis ($C+RL$). The contribution with longer effective correlation time would then be related to the rotations around the short molecular axis and to the translational diffusion modulating intermolecular interactions ($RS+D$). Close to T_{NI}, an additional contribution to T_1^{-1} appears which is caused by order fluctuations (OFs). It is easily separated from other mechanisms in view of its critical temperature dependence.

The basic difference between the relaxation mechanisms in the bulk and in the confined isotropic phase is due to the presence of the ordered surface layer. Fast molecular reorientations in the surface layer are anisotropic and do not average out intramolecular dipole-dipole proton interactions which can be therefore further modulated by slower dynamic processes. These are either fluctuations in the thickness of the boundary layer or translational diffusion of molecules among sites with different local orientational order. It was shown that the fluctuations in the thickness of the ordered layer are relevant only in a narrow temperature range up to about 1 K above the isotropic-nematic transition [37]. In our case, the difference between the relaxation rates of the bulk and confined 5CB extends over a temperature interval of more than 25 K (Fig. 3). Translational diffusion must be therefore the dominating relaxation mechanism induced by the confinement. It affects intramolecular spin interactions as the molecules migrate among the sites varying either in the degree of orientational order or in the orientation of director with respect to the magnetic field. The former process is usually addressed as the *exchange relaxation mechanism* and the latter as *reorientations mediated by translational displacements (RMTD)* [38–41].

Basic features of the spin-lattice relaxation in such a system can be evaluated within the two-phase fast-exchange model, where the first phase consists of molecules in the surface layer with restricted tumbling (order parameter $S \neq 0$) and the second one of the bulklike molecules with $S=0$. The condition of the fast exchange is fulfilled if the molecular exchange between the two phases and between different positions or orientations within the ordered phase takes place in a time which is shorter than the spin-lattice relaxation time. This condition leads to a single relaxation time of the system and manifests itself by the monoexponential relaxation curves which were in the present experiment actually observed over more than one decade.

Neglecting temporarily the intermolecular spin interactions, the spin-lattice relaxation rate induced by dipolar interaction between two protons in the same molecule is given by [36]

$$\frac{1}{T_1} = K[J_1(\omega) + 4J_2(2\omega)], \tag{2}$$

where $K=(3/20)(\mu_0/4\pi)^2\gamma^4\hbar^2/a^6$. The interproton vector of the length a is here assumed to be parallel to the long molecular axis. The functions $J_k(\omega)$ are spectral densities of the reduced autocorrelation functions $G_k(t)$ of spherical harmonics of second order, which describe the initial and final orientations of molecules relative to the external magnetic field:

$$J_k(\omega) = \int_{-\infty}^{\infty} G_k(t)\cos(\omega t)dt. \tag{3}$$

Within the two-phase model, the correlation functions are described by two partial correlation functions. The first one is related to the molecules which start at time 0 and end at time t in the surface layer, and the second one to molecules that are initially and finally in the bulklike region, regardless of the number of visits to the region of the other phase. The correlation functions of molecules that are at the beginning in one phase and at the end in the other can be neglected [38]. $G_k(t)$ is thus given by

$$G_k(t) = p_{s,s}(t)G_k(t)_{RR,RMTD} + p_{b,b}(t)G_k(t)_{IR}. \tag{4}$$

Here RR stands for the restricted reorientations of molecules in the surface layer and IR for the isotropic reorientations in the bulklike phase. The conditional probability that a molecule is initially and finally located in the surface layer is denoted by $p_{s,s}(t)$ while $p_{b,b}(t)$ stands for the conditional probability that a molecule is found initially and finally in the bulklike phase. Using rate equations for the molecular

population in each phase, it was calculated in the appendix of Ref. [38] that

$$p_{s,s}(t) = p_s(1-p_s)e^{-t/\tau_{EX}} + p_s^2 \tag{5}$$

and

$$p_{b,b}(t) = p_s(1-p_s)e^{-t/\tau_{EX}} + (1-p_s)^2, \tag{6}$$

where τ_{EX} denotes the exchange time of molecules between the surface and bulklike phases and p_s stands for the fraction of molecules in the surface layer. The translational diffusion within the ordered layer and its thickness determine the exchange time of molecules. The coefficient of translational diffusion might be close to that of the bulk isotropic phase or smaller in view of the stronger interactions between the polar liquid crystal molecules and possibly polar surface.

In describing the time dependence of the correlation functions we take into account the fact that fast molecular reorientations and the much slower RMTD process are virtually independent of each other. The total correlation function reads then

$$G_k(t) = [p_s(1-p_s)e^{-t/\tau_{EX}} + p_s^2][(1-S^2)e^{-t/\tau_{RR}} + S^2]e^{-t/\tau_{RMTD}} + [p_s(1-p_s)e^{-t/\tau_{EX}} + (1-p_s)^2]e^{-t/\tau_{IR}}. \tag{7}$$

Here τ_{RMTD} is the decay constant of the RMTD correlation and S^2 the square of the order parameter that represents the residual correlation of restricted tumbling in the long time limit, i.e., before the exchange process and RMTD become effective. Since local molecular reorientations [LR], either isotropic or restricted, are much faster than the exchange and RMTD, they definitely prevail in expressions like $1/\tau_{RMTD} + 1/\tau_{RR} \approx 1/\tau_{RR}$ or $1/\tau_{EX} + 1/\tau_{IR} \approx 1/\tau_{IR}$. The spectral density functions $J_k(\omega)$, derived from Eqs. (3) and (7), assume therefore a relatively simple form:

$$J_k(\omega) = J_k(\omega)_{LR} + J_k(\omega)_{EX,RMTD} \tag{8}$$

with

$$J_k(\omega)_{LR} = p_s(1-S^2)\frac{2\tau_{RR}}{1+\omega^2\tau_{RR}^2} + (1-p_s)\frac{2\tau_{IR}}{1+\omega^2\tau_{IR}^2} \tag{9}$$

and

$$J_k(\omega)_{EX,RMTD} = p_s(1-p_s)S^2\frac{2\tau}{1+\omega^2\tau^2} + p_s^2S^2\frac{2\tau_{RMTD}}{1+\omega^2\tau_{RMTD}^2}, \tag{10}$$

where $\tau = (1/\tau_{RMTD} + 1/\tau_{EX})^{-1}$ and $J_k(\omega) = J_1(\omega) = J_2(\omega)$. It should be mentioned that the prefactor $(1-S^2)$ in the first term of Eq. (9) is correct only in systems where the distribution of preferential molecular orientations at various surface positions is isotropic; in the nematic phase, for example, where molecules are uniformly oriented along the magnetic field, the prefactor is a linear function of S and includes the higher order parameter $\langle P_4 \rangle$ as well [36].

The description of the RMTD process with a single correlation time is often an oversimplification. The spin-relaxing capability of this process depends on the structure of the surface, i.e., on the so-called surface structure factor. The surface effect is analyzed by a spatial Fourier transformation in terms of modes with wave numbers q in the interval between $q_{\min}$ and $q_{\max}$. The correlation function for the diffusion mode with the wave number q is exponential with the decay time $\tau_q = (Dq^2)^{-1}$. Following the approach of Kimmich used in different porous media (see, for instance, Ref. [1]) we assume that in the range between $q_{\min}$ and $q_{\max}$ all modes are equally weighted, the spectral density $J_k(\omega)_{EX,RMTD}$ becomes

$$J_k(\omega)_{EX,RMTD} = \frac{p_s(1-p_s)S^2}{(\Delta q)}\int_{q_{\min}}^{q_{\max}} \frac{2(1/\tau_q + 1/\tau_{EX})^{-1}}{1+\omega^2(1/\tau_q + 1/\tau_{EX})^{-2}}dq + \frac{p_s^2S^2}{(\Delta q)}\int_{q_{\min}}^{q_{\max}} \frac{2\tau_q}{1+\omega^2\tau_q^2}dq, \tag{11}$$

where $\Delta q = q_{\max} - q_{\min}$. A closed form of Eq. (11) can be obtained in the limits $\tau_q \ll \tau_{EX}$ and $\tau_q \gg \tau_{EX}$ with the crossover between the two regimes centered at $q_c = (D\tau_{EX})^{-1/2}$. When the RMTD process is much faster than the exchange process and does not leave any residual correlation, the two terms in Eq. (11) merge into a single one, which is governed by the RMTD relaxation mechanism:

$$J_k(\omega)_{EX,RMTD} \to J_k(\omega)_{RMTD} = \frac{2^{1/2}p_sS^2}{(\Delta q)D^{1/2}}\omega^{-1/2}\left[f\left(\frac{\omega_{RMTD\max}}{\omega}\right) - f\left(\frac{\omega_{RMTD\min}}{\omega}\right)\right] \tag{12}$$

with

$$f(w) = \arctan(\sqrt{2w}+1) + \arctan(\sqrt{2w}-1) - \operatorname{arctanh}\left(\frac{\sqrt{2w}}{w+1}\right), \tag{13}$$

and $\omega_{RMTD\,\min} = Dq_{\min}^2$, $\omega_{RMTD\,\max} = Dq_{\max}^2$. Notably, the prefactor is proportional to $D^{-1/2}$ and linear in p_s. The linear dependence on p_s is characteristic for systems where the RMTD correlation function decays to zero before the molecules emerge from the ordered into the isotropic phase [16,41]. In the opposite case, i.e., in the limit of fast molecular exchange compared to the RMTD modulation, Eq. (11) turns into

$$J_k(\omega)_{EX,RMTD} \approx p_s(1-p_s)S^2\frac{2\tau_{EX}}{1+\omega^2\tau_{EX}^2} + \frac{2^{1/2}p_s^2S^2}{(\Delta q)D^{1/2}} \times \omega^{-1/2}\left[f\left(\frac{\omega_{RMTD\,\max}}{\omega}\right) - f\left(\frac{\omega_{RMTD\,\min}}{\omega}\right)\right]. \tag{14}$$

The RMTD term is here identical to that of Eq. (12) apart from the prefactor p_s^2 which enters when a molecule, being initially in the surface layer, makes several excursions into the bulklike phase before ending at time t in the surface layer again. In the simplified form with only one τ_{RMTD}, Eq. (14) is identical to the expression calculated by Burnell *et al.* for the relaxation of water in barnacle muscle, where $\tau_{RMTD} \gg \tau_{EX}$ had been assumed [38].

The RMTD spectral density function in the range between $\omega_{RMTD\,\min}$ and $\omega_{RMTD\,\max}$ is proportional to $\omega^{-1/2}$ as shown

by Eqs. (12) and (14). The low frequency cutoff $\omega_{RMTD\,\min}$ determines the turning point where $J_k(\omega)_{RMTD}$ levels off into a "plateau," independent of ω and proportional to D^{-1}:

$$J_k(\omega \to 0)_{RMTD} = \frac{2g(p_s)S^2 l_{\min} l_{\max}}{\pi^2} D^{-1}. \tag{15}$$

Here $g(p_s)$ is a function depending on the relation between τ_{EX} and τ_q, and $l_{\min} = \pi/q_{\max}$ and $l_{\max} = \pi/q_{\min}$ determine the smallest and the largest curvilinear displacements where a notable change in the orientation of the surface director is attained. A third dispersion regime occurs at frequencies above $\omega_{RMTD\max}$, where the slope of the dispersion curve becomes steeper and proportional to ω^{-2}. The spectral density in this range is given by

$$J_k(\omega \to \infty)_{RMTD} \approx \frac{2g(p_s)S^2 D\pi^2}{3\, l_{\min}^2} \omega^{-2}. \tag{16}$$

It should be stressed that the characteristic $J_k(\omega)_{RMTD} \propto \omega^{-1/2}$ behavior in the middle dispersion regime depends on the weight factors ascribed to the contributions of modes with different wave numbers q. It was shown earlier that the weight factors appropriate for diffusion restricted to a spherical cavity lead to an effective $J_k(\omega) \propto \omega^{-x}$ dependence with x ranging between 1/2 and 1. Its actual value depends on the thickness of the surface layer with respect to the cavity size and on the spatial order profile [42]. The $\omega^{-1/2}$ dependence in Eqs. (12) and (14) is characteristic for an equipartition of wave numbers describing different modes. On the other hand, Kimmich *et al.* obtained the same power-law dependence with exponent $-1/2$ also for a system of molecules strongly adsorbed to a surface with fractal dimension ~ 2.5 and obeying Levy-walk statistics [1].

IV. ANALYSIS OF EXPERIMENTAL DATA AND DISCUSSION

A brief comparison of the spin-lattice relaxation data of the bulk and confined 5CB shows that the additional relaxation mechanism in the confined state is well described by a power-law dispersion curve and is not of the BPP type. This means that the main increase in the relaxation rate upon confinement is caused by the RMTD and not by the exchange mechanism [see Eq. (14)]. The spin-lattice relaxation data are therefore quantitatively analyzed by a global target nonlinear least-square fitting minimization procedure of the model, which includes bulklike molecular dynamics, modified by the presence of ordered layer, and reorientations mediated by translational displacements (RMTD) as uncorrelated processes:

$$\frac{1}{T_1} = \left(\frac{1}{T_1}\right)_{bulk\text{-}mod.} + \left(\frac{1}{T_1}\right)_{RMTD}. \tag{17}$$

It should be stressed that in a system where both fast local molecular motions and slower reorientations mediated by translational displacements take place, the total correlation function of the system consists of the product of correlation functions related to each process [43]. Taking into account that local molecular motions are considerably faster than the RMTD process, one can assume that $G_{RMTD}(t) \sim G_{RMTD}(0)$ on the time scale on which the correlation function of local molecular motions reaches its final residual value. According to Ref. [43], this leads to Eq. (17), if the two contributions to the total relaxation rate represent *effective* contributions of the two processes. This means that $(T_1^{-1})_{bulk\text{-}mod.}$ is not the relaxation rate of the bulk liquid crystal but is modified by the presence of the ordered surface layer, and that $(T_1^{-1})_{RMTD}$ contains the residual correlation of local motions [the prefactor S^2 in Eq. (12)].

The modification of the $(T_1^{-1})_{bulk\text{-}mod.}$ term due to the presence of the ordered surface layer is the following. We assume that order fluctuations (OFs), conformational changes and molecular rotations around the long axis ($C+RL$) do not experience a significant change upon confinement. Their contribution enters into the fitting procedure with fixed parameters equal those in the bulk. On the other hand, the rate and effectiveness of hindered rotations around the short molecular axis and translational diffusion ($RS+D$) might possibly undergo a change in the ordered layer. Such a change would affect the corresponding bulk BPP contribution, i.e., the one with the longer effective correlation time. For this reason we consider the strength A and the correlation time τ_c of this term as free parameters in the fit. The RMTD relaxation mechanism is assumed to enter in the form

$$\left(\frac{1}{T_1}\right)_{RMTD} = \frac{A_{RMTD}}{\omega^{1/2}}\left[f\left(\frac{\omega_{RMTD\,\max}}{\omega}\right) - f\left(\frac{\omega_{RMTD\,\min}}{\omega}\right)\right] + \frac{4A_{RMTD}}{2^{1/2}\omega^{1/2}}\left[f\left(\frac{\omega_{RMTD\,\max}}{2\omega}\right) - f\left(\frac{\omega_{RMTD}}{2\omega}\right)\right] \tag{18}$$

where f is given by Eq. (13). In the global fit, which includes simultaneously frequency dispersions at four different temperatures and the temperature dependence at 11 kHz, we use the following adjustable parameters:

(i) The correlation time τ_c, the activation energy W, and the strength A of the $(T_1^{-1})_{bulk\text{-}mod.}$ term, and

(ii) $\omega_{RMTD\,\min}$ and $\omega_{RMTD\,\max}$ with the activation energy $-W_D$, as well as $A_{RMTD}(T)$ for the RMTD contribution.

According to Eq. (12), W_D represents the activation energy of translational diffusion. Within the two-phase fast-exchange model, A_{RMTD} is proportional to $g(p_s)S^2(\Delta q)^{-1}2^{1/2}D^{-1/2}$ [Eq. (14)]. We see that its temperature variation arises from three parameters: the fraction of ordered molecules p_s, the surface order parameter S, and the diffusion coefficient D. These parameters depend on the nature of the liquid-crystal-surface interactions, on the mutual interaction between liquid crystal molecules, and on the viscous properties of the liquid crystal. Depending on the behavior of these parameters, $A_{RMTD}(T)$ can be described by one of the following models [22,44]:

(a) The thickness of the surface layer and the surface order parameter S (constant within the layer) do not vary with temperature. The behavior of A_{RMTD} is determined by $D^{-1/2}$ alone and $A_{RMTD} \propto \exp(W_D/2k_BT)$.

(b) The order parameter has its maximum value S_0

(temperature independent) at the interface and decays then exponentially with increasing distance from the wall. The effective thickness of the ordered layer is given by the nematic correlation length, $\xi=\xi_0\sqrt{[T^*/(T-T^*)]}$, which critically increases on approaching the bulk supercooling limit T^* (usually $\sim$1 K below T_{NI}; ξ_0 is of the order of molecular length, i.e., $\sim$0.65 nm for 5CB). Within this model $A_{RMTD} \propto \exp(W_D/2k_BT)S_0^2\xi/R$, where the second factor corresponds to the product S^2p_s of the two-phase model. The above expression implies $\xi \ll R$.

(c) A thin layer of thickness l_0 with constant order parameter S_0 is located next to the wall and followed by an exponentially decaying part with the largest order parameter S_n. The thickness l_0 and the order parameters S_0 and S_n are temperature independent, whereas the decay constant ξ of the exponential part critically increases with decreasing temperature as described for model (b). A fit is thus attempted with $A_{RMTD} \propto \exp(W_D/2k_BT)(S_n^2\xi+S_0^2l_0)/R$, where the nonexponential factor again corresponds to the product S^2p_s of the two-phase model. This approximation is justified as long as the thickness of the ordered layer is smaller than the radius of the cavity, and $p_s \sim 2(\xi+l_0)/R$.

(d) The same as models (b) and (c) apart from the temperature variation of S_0 and S_n. If the order parameter in the surface layer is not determined only by the local liquid-crystal-surface interactions but predominantly by the mutual interactions among the liquid crystal molecules, it increases critically on approaching T_{NI} from above and induces a stronger temperature dependence of A_{RMTD}.

All models (a)–(d) were subsequently used in the fitting procedure in order to determine which of them provides the best description of the actual situation.

The temperature variation of $A_{RMTD} \propto \exp(W_D/2k_BT)$, which implies temperature-independent thickness of the surface layer and the order parameter S, is a good choice when applied to sample 1, but nonadequate for sample 2 as shown later.

The results of the global fit for sample 1 are presented in Figs. 4–6. The bold solid lines are obtained by fitting Eq. (17) to the experimental data. They represent the sum of four contributions, two of them are the same as in the isotropic bulk ($C+RL$ and OF), and the other two are affected ($RS+D$) or induced (RMTD) by the confinement. The contribution of order fluctuations is negligible at $\sim$10 K above the transition (Fig. 5). The fitted values of adjustable parameters are: τ_c (at 45 °C)$=4.7\times10^{-9}$ s, $W=46$ kJ/mol, $A=3.3\times10^8$ s^{-2}, $\omega_{RMTD\,\min}$ (at 45 °C)$=2\pi\times59$ kHz, $\omega_{RMTD\,\max}$ (at 45 °C)$=2\pi\times4.2$ MHz, A_{RMTD} (at 45 °C) $=1.7\times10^3$ s$^{-3/2}$, and $W_D \sim 54$ kJ/mol. Model (a) with the temperature variation of $A_{RMTD} \propto \exp(W_D/2k_BT)$ provides the best agreement between the theory and experimental data. This model implies temperature independent thickness of the surface layer and temperature independent order parameter S_0.

The analysis of experimental data for sample 2 requires a modification of the A_{RMTD} parameter. The temperature dependence of T_1^{-1} shows that—superimposed on the Arrhenius type behavior—there is also a pretransitional increasing which is not present in sample 1. This means that the thickness of the ordered layer in sample 2 is not constant and experiences at least partly a critical enhancement on approaching T_{NI}. The best agreement between the experimental data and theory is achieved by using model (c), i.e., $A_{RMTD} \propto \exp(W_D/2k_BT)(S_n^2\xi+S_0^2l_0)/R$, where the second factor corresponds to the product S^2p_s from the two-phase model. This approximation is justified as long as the thickness of the ordered layer is smaller than the radius of the cavity, and $p_s \sim 2(\xi+l_0)/R$. The solid curve in Fig. 7, resulting from the global fit of sample 2 experimental data, is plotted with $\omega_{RMTD\,\min}$ (at 45 °C)$=2\pi\times20$ kHz, $\omega_{RMTD\,\max}$ (at 45 °C) $=2\pi\times2.0$ MHz, $W_D=38$ kJ/mol, and $S_0^2l_0/S_n^2 \approx (14\pm4)$ nm.

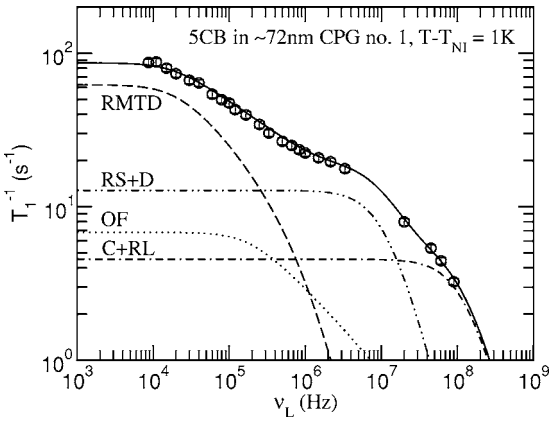

FIG. 4. Frequency dispersion of proton spin-lattice relaxation rate T_1^{-1} of 5CB in the porous glass (sample 1) at $\sim$1 K above T_{NI}. The bold solid line is a fit of Eq. (17) to the experimental data. It is a sum of four contributions: conformational changes and molecular local reorientations around the long axis ($C+RL$), molecular rotations around the short axis and translational self-diffusion ($RS+D$), order fluctuations (OFs), and reorientations mediated by translational displacements (RMTDs).

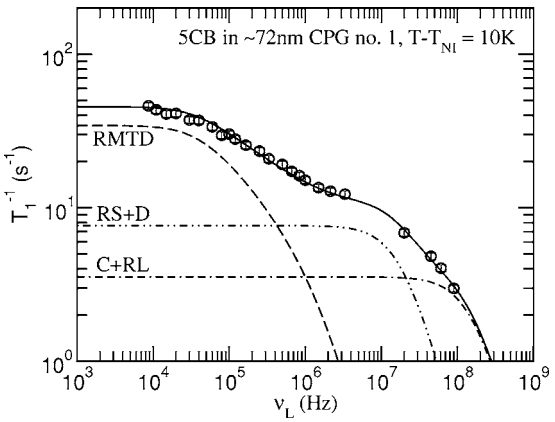

FIG. 5. Frequency dispersion of proton spin-lattice relaxation rate T_1^{-1} of 5CB in the porous glass (sample 1) at $\sim$10 K above T_{NI}. The bold solid line is a fit of Eq. (17) to the experimental data. It is a sum of four contributions: conformational changes and molecular local reorientations around the long axis ($C+RL$), molecular rotations around the short axis and translational self-diffusion ($RS+D$), order fluctuations (OFs), and reorientations mediated by translational displacements (RMTDs). The contribution of order fluctuations is negligible at this temperature.

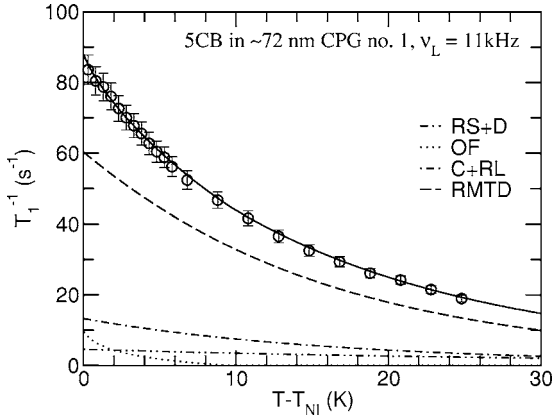

FIG. 6. Temperature dependence of proton spin-lattice relaxation rate T_1^{-1} of 5CB in the porous glass (sample 1) at Larmor frequency $\nu=11$ kHz. The bold solid line is a fit of Eq. (17) to the experimental data. RMTD is here a thermally activated process, its contribution obeys the Arrhenius law.

Other parameters do not differ appreciably from those obtained for sample 1. The value of W is close to W_D but has little impact on the global fit and cannot be accurately determined.

The best-fit parameters of the modified bulklike BPP-type relaxation contribution, ascribed to the combined effect of rotations around the short molecular axis and translational diffusion, locally modulating intermolecular spin interactions in the bulk isotropic phase $(RS+D)$, show that the correlation time of this contribution remains upon confinement practically the same as in the bulk. This does not mean, however, that there is no minor slowing down of molecular rotations next to the wall. The fitted correlation time represents an average over the whole cavity and the extensive isotropic part naturally prevails. Further we find a slight increase (smaller than 10%) in the activation energy, and an increase by a factor of about 2 in the strength A of the relaxation mechanism. The fitted correlation time allows an estimate of

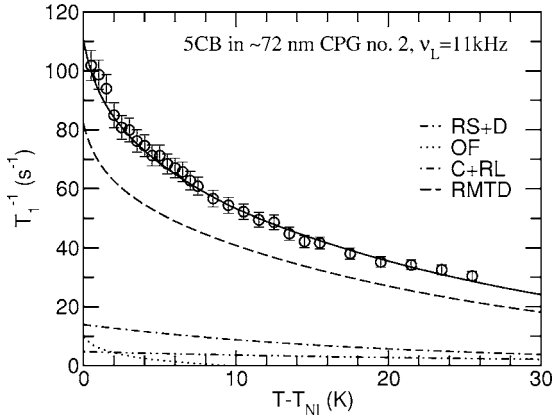

FIG. 7. Temperature dependence of proton spin-lattice relaxation rate T_1^{-1} of 5CB in the porous glass (sample 2) at Larmor frequency $\nu=11$ kHz. The bold solid line is a fit of Eq. (17) to the experimental data. The temperature dependence of RMTD contribution exhibits a pretransitional increasing superimposed on the Arrhenius-type behavior.

the mean square root displacement of the molecule within this time, i.e., $\sqrt{6D\tau_c}\approx 0.5$ nm if the bulk diffusion coefficient $D\sim 7\times 10^{-11}$ m^2/s is taken into account [45]. The estimated value corresponds to the distance between two proton spins on neighboring molecules. However, the estimated distance is also of the same order of magnitude as the thickness of a monomolecular planar layer at the interface. The enhancement in the strength of this relaxation mechanism upon confinement may therefore arise from the exchange or migration of molecules from the ordered surface layer into the bulklike phase farther away from the wall.

In the following, the best-fit values of various fitted parameters of the RMTD mechanism will be related to the structure and dynamics of the confined 5CB and discussed for both samples.

A. RMTD relaxation—frequency dispersion

Figures 4–7 show that the RMTD relaxation mechanism is overwhelmingly responsible for the increase in T_1^{-1} at low frequencies. The specific frequency dependence of $(T_1^{-1})_{RMTD}\propto\omega^{-1/2}$, anticipated by Eq. (18), provides a good description of the experimental dispersion curves. The power-law exponent $-1/2$ indicates that the CPG surface structure factor is consistent with an equipartion of different q modes. We checked the possibility of whether an exponent different from $-1/2$ would give a better fit. The test with the exponent being a free parameter yielded -0.46 for its optimum value which is pretty close to $-1/2$. Obviously, the assumption of equal weights ascribed to all modes in the range between $q_{\min}$ and $q_{\max}$ is a good approximation.

B. RMTD frequency cutoffs

The fitted values of the low and high frequency RMTD cutoffs are in the kHz and in the low MHz range, respectively. They limit the interval where the RMTD governs the time decay of correlation. The low frequency cutoff reveals itself as the inflection point in the T_1^{-1} dispersion curves marking the crossover from the low-frequency plateau to the square-root regime at intermediate frequencies. It is connected with the cutoff distance $l_{\max}=\sqrt{\pi^2 D/\omega_{RMTD\,\min}}$ which is $\sim$43 nm for sample 1 and hardly exceeds the radius of the cavity, $R\sim 36$ nm. A similar estimate of the low cutoff distance $l_{\min}$ gives $\sim$5 nm. Assuming that the diffusion might be even slower at the surface, $l_{\max}$ and $l_{\min}$ would be further diminished. These results disagree with the idealized picture of the isotropic phase in porous glasses with molecules in the surface layer aligned along the axes of elongated cylindrical cavities. The orientational correlation is obviously lost in the short time needed for a molecule to move across the cavity. The small $l_{\max}$ represents thus a strong indication that the *surface ordering is practically random planar*. Within this conjecture, $l_{\min}\sim 5$ nm might be the size of a uniformly oriented surface patch. It should be noted that the correlation function—due to the random planar structure—decays to zero before a molecule leaves the channel inhabited at time zero. Therefore the crossroads of the channels and their interconnected nature do not play a role in the proton relax-

ation. The fitted activation energy of $\omega_{RMTD\,\min}=Dq_{\min}^2$ and $\omega_{RMTD\,\max}=Dq_{\max}^2$ is ~54 kJ/mol for sample 1 and significantly exceeds the activation energy of translational diffusion in the bulk 5CB, which is only ~33 kJ/mol [45]. The larger activation energy might be associated with an attractive interaction between the solid surface and liquid crystal molecules at the interface. Such an attraction has been observed earlier for 5CB in porous glass with ~7-nm pores [46] and in sieves with ~4-nm voids [47].

The RMTD cutoff frequencies in sample 2 are smaller than in sample 1 and the limiting distances are correspondingly larger. An estimate yields $l_{\max}\sim 74$ nm and $l_{\min}\sim 7.4$ nm. Obviously, the size of uniformly oriented surface patches is larger in the sample whose CPG matrix had been exposed to a higher temperature in the preparation procedure. Larger uniformly oriented surface areas allow an extension of orientational order farther away from the orienting substrate. Interestingly, the activation energy W_D ascribed to translational diffusion is here smaller than in sample 1 and close to that of the bulk isotropic phase. It indicates that in sample 2 liquid crystal molecules which are not bonded to the surface, i.e., not residing in the first molecular layer, still possess a certain degree of orientational order and significantly contribute to the relaxation rate.

C. RMTD relaxation—temperature dependence

The variation of the RMTD relaxation with temperature deserves special attention. Apart from the thermally activated low and high frequency cutoffs, the temperature dependence of $(T_1^{-1})_{RMTD}$ is influenced also by the prefactor A_{RMTD} which reflects the shape and temperature variation of the order parameter profile. In the case that the thickness of the surface layer and the surface order parameter S do not vary with temperature, the behavior of A_{RMTD} is determined by $D^{-1/2}$ alone and therefore proportional to $\exp(W_D/2k_BT)$. Such behavior was found in sample 1. The temperature independent thickness of the surface layer supports the former conjecture, based on the small $l_{\max}$ and $l_{\min}$, that the surface alignment is random planar above T_{NI}. The randomness in the surface orientation prevents the evolution of order over distances of the nematic correlation length and implies also a temperature independent surface order parameter S, determined only by the short range interactions between the substrate and liquid crystal molecules. However, Figs. 6 and 7 show that the two samples with different treatment of the glassy matrix exhibit different temperature variations at 11 kHz. The experimental data of sample 2 are consistent with model (c) where the thickness of the ordered layer increases with decreasing temperature and where the first molecular layer at the interface has a higher degree of orientational order (S_0) than the subsequent exponentially decaying part (S_n). The fitted value of $S_0^2 l_0/S_n^2$ is $\approx(14\pm4)$ nm. Assuming the thickness $l_0\sim 2$ nm [44], it turns out that S_0 is roughly 2.5 times as large as S_n. Both order parameters are temperature independent. In the opposite case, the pretransitional increasing of $(T_1^{-1})_{RMTD}$ would be much stronger. It should be also mentioned that the function $g(p_s)$ could not be determined from the available data, i.e., the question whether the dependence of RMTD on the fraction of ordered molecules is linear or quadratic or somewhere in between is still open. This uncertainty, however, does not affect the ratio S_0/S_n which retains the same value even if the quadratic $g(p_s)$ is inserted in the fit.

The appearance of the pretransitional effects in sample 2 and their lack in sample 1 as well as the difference in the size of uniformly oriented patches demonstrate that the surface-induced liquid crystal alignment in the isotropic phase depends on the pretreatment of the CPG matrix. The difference between the aligning abilities of the two matrixes used in the present work might arise from the rests of humidity in sample 1 [48,49]. From the larger T_1^{-1} values of the sample 2, with CPG preheated to a higher temperature, we conclude that this sample has greater aligning ability for the polar 5CB resulting from less water adsorbed onto the surface OH^- groups.

V. SUMMARY

In this paper we present the measurements of the proton spin-lattice relaxation rate in the isotropic phase of liquid crystal 5CB confined into the porous glass CPG with the average diameter of pores ~72 nm. The measurements of T_1^{-1} were carried out by the fast field-cycling and conventional NMR spectrometers, and cover the frequency range from ~10 kHz to ~100 MHz. Liquid crystal 5CB has been chosen as a representative of the alkyl-cyanobiphenyl family and CPG with the average diameter of pores ~72 nm as a suitable mesoscopic confining matrix. As the NMR measurements were not performed closer to T_{NI} than at $\sim T_{NI}+0.5$ K (because of the possible temperature gradient along a relatively large sample), the critical effects observed by other methods in the immediate vicinity of T_{NI} or in smaller, nanosize cavities are not the issue of the present work.

The observed drastic increase in the spin-lattice relaxation rate of the isotropic 5CB upon confinement is quantitatively explained in terms of an additional relaxation mechanism (RMTD) and a change in the bulklike contribution to the total relaxation rate. Frequency dispersion of T_1^{-1} clearly shows that reorientations mediated by translational displacements (RMTD) produce the main, overwhelming increase in the relaxation rate. They are based on the modulation of residual spin interactions of molecules in the ordered surface layer as they diffuse among positions with different orientation of surface director. This relaxation mechanism is characterized by the nonexponential decay of correlation function leading to a specific, inverse-square-root-law dependence of relaxation rate T_1^{-1} on the Larmor frequency. Such dispersion is compatible with a surface structure imposing equal weights to diffusion modes with different wave numbers.

The low and high frequency cutoffs of the RMTD contribution limit the range where translational diffusion is responsible for the decay of correlation and throw some light on the type of surface alignment. Relatively small values of $l_{\max}$, which do not exceed the diameter of the cavity, point out that the alignment of 5CB on a glassy surface is random planar in the isotropic phase. The size of uniformly oriented patches depends on the treatment of the CPG matrix; they are of the order ~5 nm and larger in the sample that was exposed to

higher temperature in the drying procedure. The background of this phenomenon might be a small amount of water molecules attached to the glassy surface which can induce the randomness into the liquid crystal alignment. According to the size of uniformly oriented patches varies also the thickness of the surface layer. We found two different cases: in the sample with smaller oriented patches, the thickness of the ordered layer is presumably small and temperature independent; in the sample with less expressed randomness the ordered layer extends over several molecular lengths away from the surface and shows a pretransitional increase. In the latter case we observe also the existence of a first surface layer with the orientational order parameter about 2.5 times as large as in the successive boundary layer. Such an appearance in the nematogenic liquid crystal is somewhat unexpected as it used to be explained by the onset of homeotropic positional order in smectogenic compounds. It should be also noted that irrespective of the degree of randomness on the surface, the order parameter was always found to be temperature independent and obviously determined only by the short-range liquid crystal surface interactions.

The effect of confinement on the bulk BPP-type contribution with the correlation time of the order of 10^{-9} s has been investigated as well. It was found that the strength of the mechanism, i.e., the magnitude of the corresponding relaxation rate, increases by almost a factor of 2. Such an increase has been frequently *ad hoc* assumed in the analysis of deuteron transverse relaxation data in similar systems and characterized as a "relaxation mechanism with noncritical temperature dependence" [37]. The proton spin-lattice relaxometry—covering a broad frequency interval—goes farther and provides an insight into its correlation time and activation energy. The values of these two parameters indicate that the strength of one of the bulk relaxation mechanisms upon confinement might be enhanced by the exchange of molecules between the ordered layer and isotropic core of the cavity, though a definite identification of the origin of this increase is still lacking.

In this work we showed that the proton spin-lattice relaxometry at low frequencies is a sensitive method to detect the surface induced order, mainly due to the fact that the molecules in the ordered layer produce the increase in the relaxation rate upon confinement. Oppositely, the diffusion coefficient of a confined system, if measured directly by the pulsed-field-gradient NMR method, tends to be governed by less ordered environments with higher molecular mobility. A ten times smaller diffusion coefficient obtained in this way in a similar system reflects namely the tortuosity of the sample and not a possible local slowing-down of diffusion [37].

ACKNOWLEDGMENTS

The authors (G.L. and M.V.) would like to thank Professor D. Hadzi for helpful discussions. The work was supported by the Slovenian Research Agency within the program P1-0099, Bilateral Project No. BI-PT/04-06-002 and by the Portuguese Fundação para a Ciência e a Tecnologia through Project No. POCTI/ISFL/261/516. The authors also wish to thank J. Cascais and P. Fernandes of the CFMC-UL in Lisbon for their technical help with the fast field cycling NMR spectrometer.

[1] R. Kimmich and E. Anoardo, Prog. Nucl. Magn. Reson. Spectrosc. **44**, 257 (2004).
[2] W. Woelfel, F. Noack, and J. Stohrer, Z. Naturforsch. A **30a**, 437 (1975).
[3] E. Rommel, F. Noack, P. Meier, and G. Kothe, J. Phys. Chem. **92**, 2981 (1988).
[4] M. Vilfan, G. Althoff, I. Vilfan, and G. Kothe, Phys. Rev. E **64**, 022902 (2001).
[5] G. Althoff, O. Stauch, M. Vilfan, D. Frezzato, G. Moro, P. Hauser, R. Schubert, and G. Kothe, J. Phys. Chem. B **106**, 5517 (2002).
[6] J. Struppe, F. Noack, and G. Klose, Z. Naturforsch., A: Phys. Sci. **52a**, 681 (1997).
[7] R. O. Seitter, T. Link, R. Kimmich, A. Kobelkov, P. Wolfangel, and K. Mueller, J. Chem. Phys. **112**, 8715 (2000).
[8] E. Anoardo, F. Bonetto, and R. Kimmich, Phys. Rev. E **68**, 022701 (2003).
[9] A. Carvalho, P. J. Sebastião, A. C. Ribeiro, H. T. Nguyen, and M. Vilfan, J. Chem. Phys. **115**, 10484 (2001).
[10] *Liquid Crystals in Complex Geometries*, edited by G. P. Crawford and S. Zumer (Taylor & Francis, London, 1996).
[11] D. Schwarze-Haller, F. Noack, M. Vilfan, and G. P. Crawford, J. Chem. Phys. **105**, 4823 (1996).
[12] C. W. Cross and B. M. Fung, J. Chem. Phys. **99**, 1425 (1993).
[13] M. V. Terekhov, S. V. Dvinskikh, and A. F. Privalov, Appl. Magn. Reson. **15**, 363 (1998).
[14] N. Leon, J.-P. Korb, I. Bonalde, and P. Levitz, Phys. Rev. Lett. **92**, 195504 (2004).
[15] F. Grinberg, R. Kimmich, and S. Stapf, 1st Symposium on Field-cycling NMR Relaxometry, Berlin, 1998, p. 37.
[16] E. Anoardo, F. Grinberg, M. Vilfan, and R. Kimmich, Chem. Phys. **297**, 99 (2004).
[17] M. Vilfan, G. Lahajnar, I. Zupancic, and B. Zalar, Magn. Reson. Imaging **21**, 169 (2003).
[18] P. Sheng, Phys. Rev. A **26**, 1610 (1982).
[19] G. P. Crawford, D. K. Yang, S. Zumer, D. Finotello, and J. W. Doane, Phys. Rev. Lett. **66**, 723 (1991).
[20] T. Moses, Phys. Rev. E **64**, 010702(R) (2001).
[21] K. Kocevar and I. Musevic, Phys. Rev. E **65**, 021703 (2002).
[22] T. Jin, G. P. Crawford, R. J. Crawford, S. Zumer, and D. Finotello, Phys. Rev. Lett. **90**, 015504 (2003).
[23] I. Vilfan, M. Vilfan, and S. Zumer, Phys. Rev. A **40**, 4724 (1989).
[24] S. Kralj, S. Zumer, and D. W. Allender, Phys. Rev. A **43**, 2943 (1991).
[25] R. Lucht, Ch. Bahr, and G. Heppke, Phys. Rev. E **62**, 2324 (2000).
[26] M. I. Boamfa, M. W. Kim, J. C. Maan, and Th. Rasing, Nature

(London) **421**, 149 (2003).
[27] M. Vilfan, N. Vrbancic-Kopac, P. Ziherl, and G. P. Crawford, Appl. Magn. Reson. **17**, 329 (1999).
[28] G. P. Sinha, and F. M. Aliev, Phys. Rev. E **58**, 2001 (1998). In this paper it is shown that in the confined isotropic phase 5CB and its higher homologue 8CB show almost identical temperature behavior of the relaxation times of molecular rotations with only a small quantitative difference in their values.
[29] F. M. Aliev, Z. Nazario, and G. P. Sinha, J. Non-Cryst. Solids **305**, 218 (2002).
[30] M. R. Bengoechea, S. Basu, and F. M. Aliev, Mol. Cryst. Liq. Cryst. **421**, 187 (2004).
[31] A. Hourri, P. Jamee, T. K. Bose, and J. Thoen, Liq. Cryst. **29**, 459 (2002).
[32] S. Kralj, A. Zidansek, G. Lahajnar, I. Musevic, S. Zumer, R. Blinc, and M. M. Pintar, Phys. Rev. E **53**, 3629 (1996).
[33] Z. Kutnjak, S. Kralj, G. Lahajnar, and S. Zumer, Phys. Rev. E **70**, 051703 (2004).
[34] D. M. Sousa, G. D. Marques, P. J. Sebastião, and A. C. Ribeiro, Rev. Sci. Instrum. **74**, 4521 (2003).
[35] K. F. Reinhart, R. Seeliger, V. Graf, and F. Noack, J. Phys. (Paris), Colloq. **40**, C3-199 (1979).
[36] R. Y. Dong, *Nuclear Magnetic Resonance of Liquid Crystals* (Springer, New York, 1994).
[37] M. Vilfan, T. Apih, A. Gregorovic, B. Zalar, G. Lahajnar, S. Zumer, G. Hinze, R. Boehmer, and G. Althoff, Magn. Reson. Imaging **19**, 433 (2001).
[38] E. E. Burnell, M. E. Clark, J. A. M. Hinke, and N. R. Chapman, Biophys. J. **33**, 1 (1981).
[39] R. Kimmich, T. Gneiting, K. Kotitschke, and G. Schnur, Biophys. J. **58**, 1183 (1990).
[40] R. Kimmich, Chem. Phys. **284**, 253 (2002).
[41] C. Mattea, R. Kimmich, I. Ardelean, S. Wonorahardjo, and G. Farrher, J. Chem. Phys. **121**, 10648 (2004).
[42] M. Vilfan and M. Vuk, J. Chem. Phys. **120**, 8638 (2004).
[43] F. Bonetto, E. Anoardo, and R. Kimmich, J. Chem. Phys. **118**, 9037 (2003).
[44] G. P. Crawford, R. J. Ondris-Crawford, J. W. Doane, and S. Zumer, Phys. Rev. E **53**, 3647 (1996).
[45] S. V. Dvinskikh, I. Furo, H. Zimmermann, and A. Maliniak, Phys. Rev. E **65**, 061701 (2002).
[46] Ch. Cramer, Th. Cramer, F. Kremer, and R. Stannarius, J. Chem. Phys. **106**, 3730 (1997).
[47] I. Gnatyuk, G. Puchkovska, I. Chashechnikova, F. Nozirov, S. Jurga, and B. Peplinska, J. Mol. Struct. **700**, 183 (2004).
[48] See, e.g., V. N. Naraev, Glass Phys. Chem. **30**, 367 (2004).
[49] Y. Morimoto, T. Igarashi, H. Sugahara, and S. Nasu, J. Non-Cryst. Solids **139**, 35 (1992).